Long-Lived Ultrafast Spin Precession in Manganese Alloys Films with a Large Perpendicular Magnetic Anisotropy

S. Mizukami,[1,*] F. Wu,[1] A. Sakuma,[2] J. Walowski,[3] D. Watanabe,[1] T. Kubota,[1] X. Zhang,[1] H. Naganuma,[2] M. Oogane,[2] Y. Ando,[2] and T. Miyazaki[1]

[1]WPI-Advanced Institute for Materials Research, Tohoku University, Sendai 980-8577, Japan
[2]Department of Applied Physics, Tohoku University, Sendai 980-8579, Japan
[3]I. Physikalisches Institut, Universittät Göttingen, 37077 Göttingen, Germany
(Received 24 August 2010; published 16 March 2011)

Spin precession with frequencies up to 280 GHz is observed in $Mn_{3-\delta}Ga$ alloy films with a perpendicular magnetic anisotropy constant $K_u \sim 15$ M erg/cm^3. The damping constant α, characterizing macroscopic spin relaxation and being a key factor in spin-transfer-torque systems, is not larger than 0.008 (0.015) for the $\delta = 1.46$ (0.88) film. Those are about one-tenth of α values for known materials with large K_u. First-principles calculations well describe both low α and large K_u for these alloys.

DOI: 10.1103/PhysRevLett.106.117201 PACS numbers: 75.78.Jp, 75.50.Vv, 75.70.Tj, 76.50.+g

Spin dynamics and relaxation in magnetic metals are of fundamental importance in spintronics. They are phenomenologically well described by the Landau-Lifshitz-Gilbert equation $\dot{\mathbf{M}} = -\gamma \mathbf{M} \times \mathbf{H}_{\rm eff} + (\alpha/M_S)\mathbf{M} \times \dot{\mathbf{M}}$, where $\mathbf{M}$ is the magnetization vector, γ the gyromagnetic ratio, $\mathbf{H}_{\rm eff}$ the effective magnetic field, and M_S the saturation magnetization [1]. The second term on the right-hand side of the equation describes the macroscopic spin relaxation, namely, Gilbert damping. The factor α is the dimensionless damping constant that determines the macroscopic spin relaxation time $\tau \sim 1/(2\pi\alpha f)$ for the spin precession with frequency f. Furthermore, α is one of the key factors in spin-transfer-torque systems [2].

Previous studies have indicated that the damping originates from electronic transitions induced by the spin-orbit (SO) interaction [3], similar to the Elliot-Yafet spin relaxation mechanism in metals and semiconductors [4]. In the simplest expression, $\alpha \sim [\mu_B^2 D(E_F)/\gamma M_S](\xi/W)^2/\tau_E$, where $D(E_F)$ is the density of states at the Fermi level E_F, ξ the SO interaction energy, W the d-band width, and $1/\tau_E$ the electron scattering frequency [5,6]. Subsequent experiments have supported the above relation for α qualitatively in *soft* magnetic alloys [7–9]. A quantitative theory has been developed based on the torque-correlation model [6] using first-principles band structure calculations that predicted the correct orders of magnitude for α of Fe, Co, and Ni [10] and demonstrated the influence of density of states on α in half-metallic magnets [9,11].

On the other hand, the damping mechanism in metallic magnets with large uniaxial magnetic anisotropy constant K_u is unknown yet. The K_u also includes second-order SO interaction effects [12]; thus, alloys with large K_u may have large α, which is consistent with experimental results. Recently reported values for α range from 0.04 to 0.4 for films with large K_u, e.g., Co-based multilayers, ultrathin films, and hcp CoCrPt alloys [13–19]. Those are about 10 times larger than α in Fe-Co-Ni alloys. However, the question is still open whether a low α is compatible with a large K_u or there is a correlation between those two in metallic magnets, as has been pointed out in a different context [20]. This question should be clarified to understand the damping mechanism more profoundly. Meanwhile, the search for materials with both large K_u and low α is urgently motivated by practical applications, such as high-density spin memory devices controlled by the spin-transfer torque [2].

In this Letter, we report the observation of spin precession in Mn-Ga alloy films with large K_u by using the time-resolved magneto-optical Kerr effect, demonstrating the compatibility of large K_u and low α. Although the elements Mn and Ga are nonmagnetic, two phases of its composed alloy $Mn_{3-\delta}Ga$ show strong magnetism with high Curie temperatures up to ~800 K. The first one, the so-called δ phase, has a tetragonal $L1_0$ structure and is stable for $\delta \cong 1$–2 [21]. The second phase is a tetragonal $D0_{22}$ structured alloy, appearing when $\delta \leq 1$ [22]. It was predicted to be a Heusler-like compound with high spin polarization at $\delta = 0$ [23]. While Mn and Ga are light elements with a low SO interaction, both phases exhibit large K_u with an easy axis parallel to the c axis [21,22].

The 100-nm-thick epitaxial $Mn_{3-\delta}Ga$ alloy films were grown on (100)-MgO single crystal substrates at deposition temperatures of 450–500 °C by using magnetron sputtering with a base pressure lower than 10^{-6} Pa and an Ar pressure of 0.1 Pa. The films were capped with a 1-nm-thick protective Ta layer after cooling down to room temperature. Films with $\delta = 1.46$ and 0.88, as determined by Rutherford backscattering spectroscopy, were prepared because stoichiometric films ($\delta = 0, 2$) with better qualities were difficult to grow. From $\omega - 2\theta$ and pole figure x-ray diffraction measurements, the epitaxial relationship was determined to be MgO(001)$\langle 100 \rangle \| Mn_{3-\delta}Ga(001)\langle 100 \rangle$. The film with $\delta = 1.46$ (0.88) is a $L1_0$ ($D0_{22}$) ordered structure, identified from the presence of superlattice peaks for (001) and (101), respectively [22]. The long-range ordering parameters are close to 90% of maximum ordering at the respective compositions, estimated from the integrated intensity ratio of the superlattice and fundamental peaks. The respective lattice constants are $(a, c) = (3.91\ \text{Å}, 3.60\ \text{Å})$ and $(a, c) = (3.92\ \text{Å}, 7.11\ \text{Å})$ for $\delta = 1.46$ and 0.88. The rocking curve width of the (002) peak for $\delta = 1.46$ [the (004) for $\delta = 0.88$] is $\sim 0.5°$ (see details in Ref. [24]).

Figure 1(a) shows typical hysteresis curves for $\delta = 1.46$, measured by using a superconducting quantum interference device magnetometer. The magnetization M exhibits a perpendicular remanent magnetization when magnetic field H is applied perpendicular to the film plane. The estimated M_S is 500 (305) emu/cm^3 for the $\delta = 1.46$ (0.88) film, comparable to those reported previously [25].

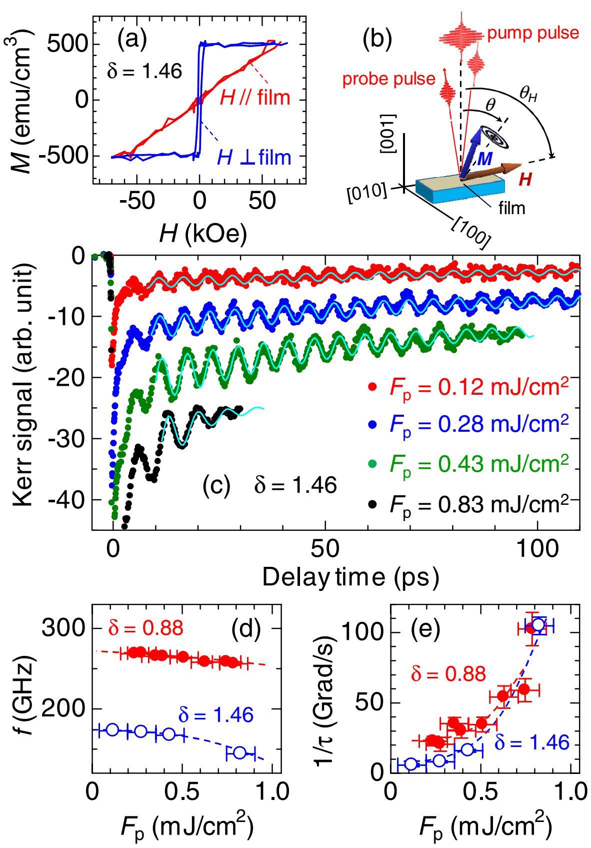

FIG. 1 (color online). (a) Typical hysteresis curves for the $Mn_{3-\delta}Ga$ epitaxial film with $\delta = 1.46$. (b) Schematic of the time-resolved magneto-optical Kerr effect measurement geometry. The applied magnetic field H was directed at an angle θ_H with respect to the film normal. Spin precession occurs around the equilibrium angle θ of magnetization M. (c) Typical time-resolved Kerr signals for the $\delta = 1.46$ film with different pump fluences F_p at $\theta_H = 80°$ and $H = 10.4$ kOe. The solid curves show the fitted data. (d) Precession frequency f and (e) inverse relaxation time $1/\tau$ for the films with $\delta = 1.46$ (○) and 0.88 (●) as functions of F_p. The dashed curves are visual guides only.

The effective perpendicular magnetic anisotropy field H_k^{eff} is estimated to 60 (86) kOe for the $\delta = 1.46$ (0.88) film. The K_u values are around 15 M erg/cm^3 for both films, evaluated from the relation $K_u = M_S H_k^{\text{eff}}/2 + 2\pi M_S^2$.

Time-resolved Kerr signals were measured in a conventional all-optical pump-probe setup using a Ti:sapphire laser with a regenerative amplifier. The s-polarized probe and pump beams have respective beam spot sizes of 0.77 and 2.0 mm. The incident light is almost perpendicular to the film plane, and the Kerr signal is proportional to the out-of-plane component of magnetization, as illustrated in Fig. 1(b) (see details in Ref. [26]), and thus the changes of Kerr signal owing to spin precession increase with increasing field angle θ_H. Figure 1(c) shows typical time-resolved Kerr signals for the film with $\delta = 1.46$ using different pump fluences F_p at $H = 10.4$ kOe and $\theta_H = 80°$, the maximum angle in our setup, from the film normal [Fig. 1(b)]. The Kerr signals exhibit oscillations following rapid decreases at zero delay time [Fig. 1(c)] [26]. Oscillation amplitude becomes larger with increasing F_p, while oscillation frequency and decay time noticeably decrease, indicating that the oscillatory signals are induced by the pump beams. In the lower F_p regime, the oscillations are very fast and do not decay significantly, in contrast to those observed in Co/Pt multilayers with high K_u [13].

Additionally, we examined time-resolved Kerr signals for the films by varying H at $\theta_H = 80°$ (not shown here). The oscillation amplitude and frequency in the Kerr signals decrease with decreasing H, and the oscillation amplitude is comparable to the noise at $H = 4.2$ kOe. These observations confirm that the oscillations in the Kerr signals originate from spin precession in the films, because the angle θ between M and the film normal [Fig. 1(b)] decreases with decreasing H and the out-of-plane component of spin precession becomes smaller.

Figures 1(d) and 1(e) depict, respectively, the F_p dependence of f and $1/\tau$ for both films, extracted by fitting an exponentially damped sine function to the time-resolved Kerr signal [solid curves in Fig. 1(c)], as described in Ref. [15]. The f and $1/\tau$ show remarkable variation with F_p, which can be ascribed to the rising temperature and nonlinear spin excitations, while the increase of f and decrease of $1/\tau$ become smaller with lowering F_p, corresponding to spin dynamics in the small-angle precession regime at near ambient temperature.

Figures 2(a) and 2(b) show the time-resolved Kerr signals for both films with different θ_H, measured at $H = 10.4$ kOe and $F_p = 0.12$ (0.28) mJ/cm^2 corresponding to $\delta = 1.46$ (0.88). The signals clearly show a variation of the precession period, when varying θ_H. Figure 2(c) shows the dependency of f on θ_H. The f values decrease as θ_H increases. A similar behavior can also be observed for films with lower K_u [15,19]. For a quantitative analysis of the precessional dynamics we use the expression

$f = (\gamma/2\pi)\sqrt{H_1H_2}$ with $H_1 = H\cos(\theta_H - \theta) + H_k^{\rm eff}\cos^2\theta$ and $H_2 = H\cos(\theta_H - \theta) + H_k^{\rm eff}\cos 2\theta$ for a uniform precession around the equilibrium direction θ for a small cone angle, derived from the Landau-Lifshitz-Gilbert equation by using the condition $\alpha \ll 1$. The angle θ is computed concurrently by using $\sin 2\theta = (2H/H_k^{\rm eff})\sin(\theta_H - \theta)$ [19]. By assuming the Landé g factor of $g = 2.0$ and adjusting $H_k^{\rm eff}$, theoretical values for f vs θ_H were fitted to the experimental data [solid curves in Fig. 2(c)]. The best fit $H_k^{\rm eff}$ value is 61 (95) kOe for the $\delta = 1.46$ (0.88) film and is comparable to that estimated from the hysteresis curves. The uncertainty of the best fit $H_k^{\rm eff}$ values is inferred to be $\sim$10% because the value of g ranges from 2.0 to 2.2 in transition-metal magnets [3]. To our knowledge, there are no reports on ultrafast uniform spin precession with precession frequencies as high as 280 GHz in metallic magnets, stemming from a large anisotropy field, so far. Similarly, the θ_H dependencies of $1/\tau$ are derived and plotted in Fig. 2(d). The $1/\tau$ values are almost independent of θ_H for both films within the experimental errors. These are in agreement with $1/\tau$ values calculated by using the equation $1/\tau = 2\pi\alpha f P$ for uniform precession with $\alpha = 0.006$ (0.016) for $\delta = 1.46$ (0.88) films [solid curves in Fig. 2(d)], where $P = \gamma(H_1 + H_2)/4\pi f$ is the precession ellipticity factor [19]. Experimental errors in $1/\tau$ cannot exclude extrinsic spin relaxation mechanisms [19], and thus we also consider the effective damping constant $\alpha_{\rm eff}$, defined at each θ_H by the relation $\alpha_{\rm eff} = 1/2\pi f\tau$ and plotted in Fig. 2(e). The $\alpha_{\rm eff}$ is not the intrinsic α but the quantity accounting for the extrinsic spin relaxation attributed to such processes as two-magnon scattering and anisotropy dispersion [17]. Thus, $\alpha_{\rm eff}$ determines an upper bound for the true α [19]. Typical values of $\alpha_{\rm eff}$ for the $\delta = 1.46$ and 0.88 films are 0.0053 ± 0.001 and 0.014 ± 0.003, respectively, at $\theta_H = 80°$, with respective averaged values of 0.0075 ± 0.003 and 0.015 ± 0.003. The $\alpha_{\rm eff}$ values reported here approximate α values for materials with weak magnetic anisotropy, i.e., Fe, Co, and Ni [7] [dashed lines in Fig. 2(e)].

In order to examine the experimental α and K_u, theoretical calculations in stoichiometric and ordered $L1_0$ MnGa and $D0_{22}$ Mn_3Ga were performed. Spin-polarized band structures were calculated with linear muffin-tin orbitals in the atomic sphere approximation based on the density functional formalism using lattice constants of $a =$ 3.92 Å (3.91 Å) and $c = 3.55$ Å (7.17 Å) for $L1_0$ MnGa ($D0_{22}$ Mn_3Ga). The density of states profiles [Fig. 3(a)] and magnetic moments for the alloys are almost identical to those in Refs. [23,27]. The calculation of K_u using the linear muffin-tin orbitals in the atomic sphere approximation including the SO interaction and the force theorem [28] yielded $\sim$20 M erg/cm^3 for both alloys, in excellent agreement with the experimental K_u. The α was computed by using the torque-correlation model [6,10] based on the results from first-principles calculations mentioned above.

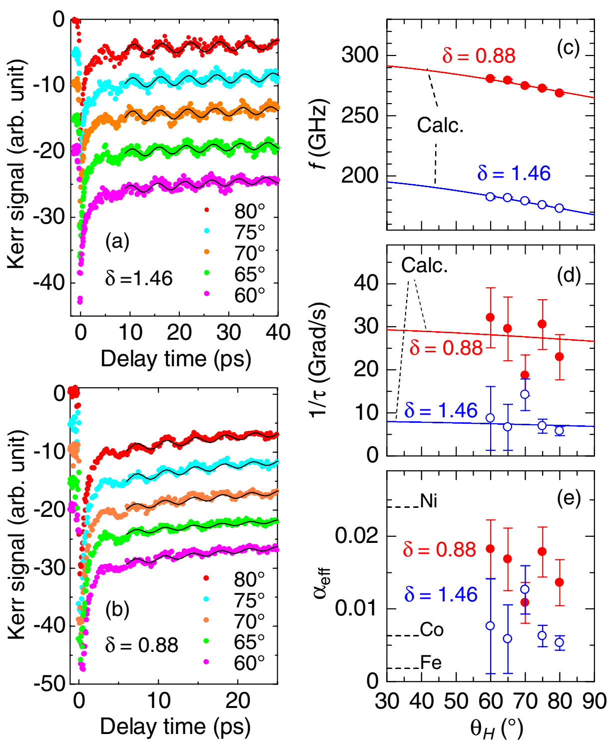

FIG. 2 (color online). Magnetic field angle θ_H variation of time-resolved Kerr signals in the epitaxial films of $Mn_{3-\delta}Ga$ with $\delta = 1.46$ (a) and 0.88 (b), where the solid curves show the fit to the data. The data are shifted for clarity. The θ_H dependence of spin precession frequency f (c), inverse relaxation time $1/\tau$ (d), and effective damping constant $\alpha_{\rm eff}$ (e). The open (filled) circles correspond to the data for $\delta = 1.46$ (0.88). The solid curves through data points are model fits. The dashed lines in (e) show typical damping constants α for Fe, Co, and Ni [7].

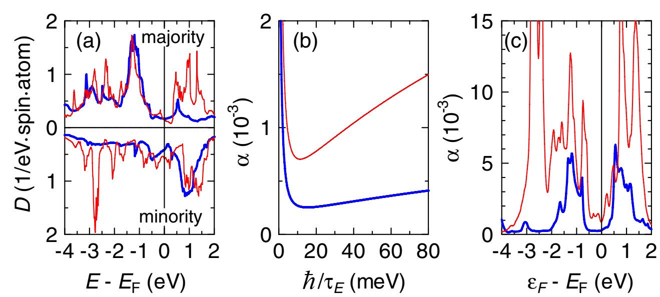

FIG. 3 (color online). Theoretical calculations of (a) density of states and (b) damping constant α as a function of electron scattering frequency $\hbar/\tau_E$ in units of eV. (c) Theoretical calculations of damping constant with shifting Fermi energy ϵ_F from E_F, based on the band structure corresponding to (a) with different band fillings. The E_F is the Fermi energy corresponding to the valence electron number of Mn-Ga alloys. In (c), the calculation was performed at $\hbar/\tau_E = 26$ meV that corresponds to thermal broadening at 300 K. The thick (thin) curve corresponds to the data for stoichiometric and ordered $L1_0$ MnGa ($D0_{22}$ Mn_3Ga).

Figure 3(b) displays the dependence of theoretical α for $L1_0$ MnGa and $D0_{22}$ Mn_3Ga alloys on $\hbar/\tau_E$, showing a minimum at $\hbar/\tau_E \sim 10$ meV. These minima originate from the combination of inter- and intraband transition [10]. The theoretical α values in $D0_{22}$ Mn_3Ga are close to those for Fe and Co, already calculated by us and others [10]. In contrast, α values for $L1_0$ MnGa are all lower than for $D0_{22}$ Mn_3Ga [Fig. 3(b)]. Although the theoretical α at ambient temperature ($\hbar/\tau_E = 26$ meV) is smaller by a factor of 10 than $\alpha_{\rm eff}$ for the films, we consider that these theoretical results agree qualitatively with the experiment at this stage if we take into account the high resistivity ($\sim 130\ \mu\Omega$ cm), the off-stoichiometric composition, and the possibility that $\alpha_{\rm eff}$ is larger than the true α for the films.

To understand the small α, we further calculated α by shifting the Fermi energy ϵ_F from E_F of Mn-Ga alloys using the torque-correlation model [Fig. 3(c)] [29], based on the band structures corresponding to Fig. 3(a) with different band fillings. The α shows a minimum at E_F but increases rapidly when ϵ_F is shifted by $\sim$0.5 eV above and below E_F, reflecting the density of states near E_F [Fig. 3(a)]. This can be understood qualitatively in analogy to the relation $\alpha \propto \xi^2 D(\epsilon_F)$, as mentioned above. Therefore, the low α is likely attributable to the low $D(E_F)$ for Mn-Ga alloys, analogous in part to Heusler and related alloys [8,9,11]. The calculated ξ for Mn d orbitals was $\sim$40 meV, being as small as those for the other 3d elements and also favorable for the low α.

The K_u was also calculated as a function of the band filling q to consider why K_u is large in these alloys with the small ξ [27,30]. The K_u value oscillates against q between negative and positive values and exhibits a positive maximum at the valence electron numbers for the Mn-Ga alloys. Thus, the large K_u is not solely related to the SO interaction but also depends strongly on electronic structure near E_F formed by the tetragonal and layered atomic structure in Mn-Ga alloys, similarly to Ni/Co multilayers or tetragonal FeCo alloys with large K_u [31,32]. A detailed analysis based on band structures is lengthy and will be described elsewhere.

In summary, we investigated spin dynamics in the epitaxial $Mn_{3-\delta}Ga$ alloy films. The K_u value for the films was $\sim$15 M erg/cm^3, and the α value for the film with $\delta = 1.46$ (0.88) was not larger than 0.008 (0.015). Both high K_u and low α were explained qualitatively by first-principles calculations. The result deepens the understanding of the underlying physics of damping in magnetic metals and also gives instructive indications on the design of materials with these properties.

This work was partially supported by Grant for Industrial Technology Research from NEDO, Strategic International Cooperative Program from JST, Grant-in-Aid for Scientific Research from JSPS, the Asahi glass foundation, and DAAD (J. W.).

*mizukami@wpi-aimr.tohoku.ac.jp

[1] T. L. Gilbert, IEEE Trans. Magn. **40**, 3443 (2004).
[2] S. Mangin *et al.*, Appl. Phys. Lett. **94**, 012502 (2009).
[3] Z. Frait and D. Fraitová, in *Spin Wave and Magnetic Excitations*, edited by A. S. Borovik-Romavov and S. K. Shinha (North-Holland, Amsterdam, 1988); B. Heinrich, in *Ultrathin Magnetic Structures III*, edited by J. A. C. Bland and B. Heinrich (Springer-Verlag, Berlin, 2005).
[4] I. Žutić, J. Fabian, and S. Das Sarma, Rev. Mod. Phys. **76**, 323 (2004).
[5] V. Kamberský, Can. J. Phys. **48**, 2906 (1970).
[6] V. Kamberský, Czech. J. Phys., Sect. B **26**, 1366 (1976).
[7] D. Bastian and E. Biller, Phys. Status Solidi A **35**, 113 (1976); F. Schreiber *et al.*, Solid State Commun. **93**, 965 (1995); J. Pelzl *et al.*, J. Phys. Condens. Matter **15**, S451 (2003); S. Ingvarsson *et al.*, Appl. Phys. Lett. **85**, 4995 (2004); J. O. Rantschler *et al.*, J. Appl. Phys. **101**, 033911 (2007).
[8] S. Mizukami *et al.*, J. Appl. Phys. **105**, 07D306 (2009); M. Oogane *et al.*, Appl. Phys. Lett. **96**, 252501 (2010).
[9] H. Lee *et al.*, Appl. Phys. Lett. **95**, 082502 (2009).
[10] K. Gilmore, Y. U. Idzerda, and M. D. Stiles, Phys. Rev. Lett. **99**, 027204 (2007).
[11] C. Liu *et al.*, Appl. Phys. Lett. **95**, 022509 (2009).
[12] P. Bruno, in *Magnetismus von Festköpern und Genzflächen*, edited by P. H. Dederichs, P. Grünberg, and W. Zinn (Forschungszentrum, Jülich, 1993).
[13] A. Barman *et al.*, J. Appl. Phys. **101**, 09D102 (2007).
[14] G. Malinowski *et al.*, Appl. Phys. Lett. **94**, 102501 (2009).
[15] S. Mizukami *et al.*, Appl. Phys. Lett. **96**, 152502 (2010).
[16] Y. Nozaki *et al.*, Appl. Phys. Lett. **95**, 082505 (2009).
[17] J.-M. Beaujour *et al.*, Phys. Rev. B **80**, 180415 (2009).
[18] N. Inaba *et al.*, IEEE Trans. Magn. **33**, 2989 (1997).
[19] S. Mizukami *et al.*, Appl. Phys. Express **3**, 123001 (2010).
[20] D. Steiauf and M. Fähnle, Phys. Rev. B **72**, 064450 (2005).
[21] T. A. Bither and W. H. Cloud, J. Appl. Phys. **36**, 1501 (1965).
[22] H. Niida *et al.*, J. Appl. Phys. **79**, 5946 (1996).
[23] B. Balke *et al.*, Appl. Phys. Lett. **90**, 152504 (2007).
[24] F. Wu *et al.*, Appl. Phys. Lett. **96**, 042505 (2010); see also supplemental material at http://link.aps.org/supplemental/10.1103/PhysRevLett.106.117201 for the structural analysis.
[25] K. M. Krishnan, Appl. Phys. Lett. **61**, 2365 (1992); F. Wu *et al.*, Appl. Phys. Lett. **94**, 122503 (2009).
[26] M. van Kampen *et al.*, Phys. Rev. Lett. **88**, 227201 (2002).
[27] A. Sakuma, J. Magn. Magn. Mater. **187**, 105 (1998).
[28] A. Sakuma, J. Phys. Soc. Jpn. **63**, 1422 (1994).
[29] K. Gilmore, Y. U. Idzerda, and M. D. Stiles, J. Appl. Phys. **103**, 07D303 (2008).
[30] See supplemental material at http://link.aps.org/supplemental/10.1103/PhysRevLett.106.117201 for the calculated data of K_u vs q in the alloys.
[31] G. H. O. Daalderop, P. J. Kelly, and F. J. A. den Broeder, Phys. Rev. Lett. **68**, 682 (1992).
[32] T. Burkert *et al.*, Phys. Rev. Lett. **93**, 027203 (2004).